Optical Materials: X 12 (2021) 100120

Contents lists available at ScienceDirect

Optical Materials: X

journal homepage: www.journals.elsevier.com/optical-materials-x

Invited Review Article

Phoxonic glass cavities based on whispering gallery mode resonators

D. Farnesi [a], S. Berneschi [a], G. Frigenti [a], G. Nunzi Conti [a,*], S. Pelli [a], P. Feron [b], T. Murzina [c], M. Ferrari [d], S. Soria [a]

[a] Institute of Applied Physics "N. Carrara", Italian National Research Council, CNR-IFAC, Via Madonna del Piano 10, 50019, Sesto Fiorentino, Italy
[b] ENSSAT-FOTON (CNRS-UMR 6082), Université de Rennes 1, 6 rue de Kerampont, 22300, Lannion, France
[c] Department of Physics, M.V. Lomonosov Moscow State University, Leninskie Gory,1, 62, Moscow, 119991, 11, Russia
[d] IFN-CNR CSMFO Lab. and FBK Photonics Unit, Via alla Cascata 56/C, 38123, Povo, Italy

ARTICLE INFO

Keywords:
Whispering gallery modes
Optical resonators
Microspheres
Microbubbles
Lasers
Non-linear optics
Brillouin scattering
Polymer coatings
Optical switching

ABSTRACT

A variety of studies have been performed on WGM microresonators made of different materials and exploiting very high quality factors. This feature has allowed their use in a broad variety of applications including micro-lasers, optical filtering and switching, frequency conversion through non-linear effects, RF photonics and sensing. The easiest way to shape a glass spheroid with high quality factor is to use the surface tension during the thermal reflow of a highly transparent amorphous dielectric. Depending on the application, alternatives shapes like micro-bubbles or micro-bottles can be implemented in order to obtain specific performances. This manuscript reports the results we obtained on micro-laser sources in erbium doped microspheres, parametric frequency conversion in silica microspheres, stimulated Brillouin scattering in silica microbubbles, and non-linear effects in polymer coated or fluorophore filled glass microcavities.

1. Introduction

Since the first demonstration of high Q factor ($Q \geq 10^8$) fused quartz WGM micro-resonator [1] a large number of studies have been performed on glass based resonators in many fields including micro-lasers [2,3], non-linear optics [4], optomechanics [5], sensing [6–8] and RF photonics [9]. The narrow resonant-wavelength lines and high energy density [10] are attractive characteristics that make these miniaturized resonators suitable not only for practical applications but also for the investigation of fundamental processes [11,12]. Solid and hollow resonators, such as microspheres [13], microbubbles [14] and microbottles [15,16] have been extensively used with excellent application performances. WGM microresonators can be made by means of surface tension during the thermal reflow of a low loss amorphous glassy dielectric, which allows shaping high-surface-quality spheroids. The glass melting temperature is reached by using CO_2 lasers, a flame, micro-heaters, or electric arcs [17]. These heating source can be applied to the tip of a fiber or of a glass stem and also to the powder obtained by crushing the glass [13] in order to obtain spherical shapes. Microbubble resonators can be fabricated from glass capillaries with a similar melting process and at the same time applying an internal pressure to isotropically expand them [18]. Various glasses, beside silica or silicate, can be used to fabricate resonators with enhanced properties in terms of non-linear effects [19], transparency windows [20,21] and ability to host rare earths [22]. In this paper we review the main results we have obtained studying lasing and non-linear effects in glass microresonator, exploiting micro-laser sources in erbium doped glass microspheres, and parametric and non-parametric effects in silica microspheres and microbubbles. Indeed, hollow WGM resonators proved to be efficient phoxonic cavities, meaning that they can sustain both photons and phonons, either optical or acoustic [23]. Finally, either polymer coated silica microspheres or fluorophore filled microbubbles have been studied in order to add specific functionalities to the resonator.

2. Erbium doped microSPHERES as laser sources

Two different approaches have been exploited for microspheres fabrication from three different types of Er^{3+}doped, Yb^{3+}-codoped glasses: a potassium-barium-alumino phosphate glass (Schott IOG2) with 2 wt% of Er_2O_3 and 3 wt% of Yb_2O_3, a sodium-alumino-phosphate glass (Schott IOG1) with contains 1.5 wt% of Er_2O_3 and 3 wt% of Yb_2O_3, and a silicate glass (Schott IOG10), with 1 wt% of Er_2O_3 and 8 wt% of Yb_2O_3. In the first fabrication method a plasma torch, generated using a microwave supply, melts the pieces of each bulk glass which were

* Corresponding author.
E-mail address: g.nunziconti@ifac.cnr.it (G. Nunzi Conti).

https://doi.org/10.1016/j.omx.2021.100120
Received 29 October 2021; Received in revised form 12 November 2021; Accepted 13 November 2021
Available online 19 November 2021

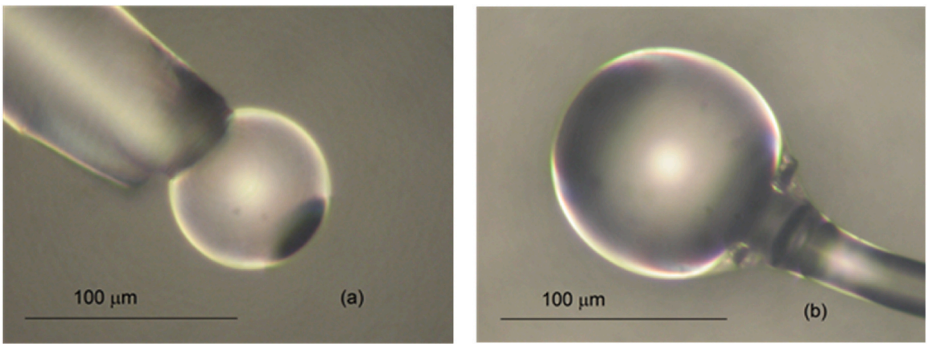

Fig. 1. a) Image of an IOG-1 microsphere glued to the tip of a fiber. b) Image of a microsphere fabricated by directly melting the tip of an IOG-1 glass stem.

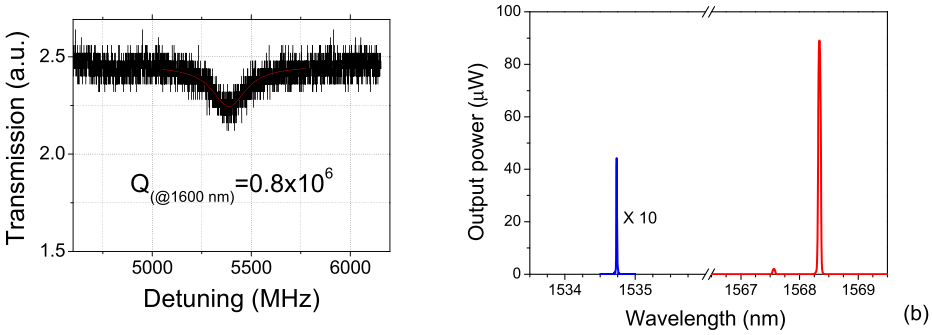

Fig. 2. a) WGM undercoupled resonance around 1600 nm corresponding to a *Q* factor of 0.8 × 10^6 for a 75 μm microsphere in IOG1 glass, b) WGMs laser spectra from the same sphere. At 1568.3 nm (red line) a peak power of 90 μW obtained using a pump power of 6.1 mW and at 1534.7 (blue line) a peak of about 5 μW. (For interpretation of the references to color in this figure legend, the reader is referred to the Web version of this article.)

ground first and then injected axially through the plasma, while the surface tension gives them their spherical shape [24]. The microsphere diameters, which depend mainly on the powder size, were selected in the range between 50 μm and 100 μm. As shown in Fig. 1a, the spheres are then glued to the cleaved tip of a tapered optical fiber for easy handling. In the second approach, IOG1 wafers were cut in 5 cm long rods of 1.5 mm square cross section which were then drawn in a home-made pulling system. A glass thread with a diameter in the range 10 μm–30 μm and a length of 2 cm is obtained. An oxygen-butane torch was slowly approached to the tip of the thread in order to form the microsphere. This fabrication system was encased in a nitrogen saturated atmosphere. Spheres with diameters in the range between 60 μm and 120 μm are obtained depending on the glass thread diameter and the exposition time [25]. Fig. 1b shows a microsphere with a diameter of 100 μm attached to the fiber stem from which it is made.

The laser characterization was performed at pumping wavelength of 1480 nm for exciting Er^{3+} ions so that the best mode and phase matching condition, at both the pump and the laser wavelengths, can be fulfilled for the WGMs [26]. A fiber stabilized laser (Corning Lasertron) or a narrow-line tunable laser diode (TLD; Anritsu Tunics) are injected in a home-made biconical tapered fiber to excite microsphere WGMs and, at the same time, to couple the fluorescence or laser light out of the resonator. Finally, the co-propagating signal and the fluorescence were sent to an optical spectrum analyzer (OSA, Ando AQ6317B). We demonstrate lasing action with pump threshold in the mW range for all types of microspheres. The pump power has been considered as the difference between the launched one and the one collected at the taper output after the resonator. Microspheres fabricated from glass powder of IOG1 glass [25] present the best performances. Fig. 2a shows the typical *Q* factor (close to 10^6) measured outside the Er^{3+} absorption band. Lasing occurred both in single mode and multimode conditions by increasing the pump power above a minimum threshold of about 1 mW. The maximum output power of 90 μW at 1568.3 nm, with a pump power of 6.1 mW at 1480 nm, is shown in Fig. 2b. The variation of relative position between the taper and the sphere, and the increase of pump power can affect the lasing spectrum which will move towards lasing modes at shorter wavelength. This effect allows wavelength tunability in excess of 30 nm (Fig. 2b), and relates to the shift in the Er^{3+} gain spectrum that occurs when the inversion rate increases [24].

3. Parametric and non-parametric oscillations in silica WGMR

High Q WGM resonators are a unique platform for nonlinear wave generation at low power continuous wave, which represent one of the biggest challenges in nonlinear optics. Parametrical processes – including harmonic generation, third-order sum-frequency generation (TSFG), four wave mixing (FWM) and coherent anti-Stokes Raman spectroscopy (CARS) – are predominant for non or near resonant interactions, where the initial and final quantum states are the same, which means that there is no real material absorption of photons. Their process lifetimes are extremely short (less than a femtosecond) because they involve only virtual energy levels. On the other hand, non-parametric processes – including Stimulated Raman Scattering (SRS) and Stimulated Brillouin Scattering (SBS) – involve real energy levels with different initial and final quantum states. The energy transfer from the photons to the host medium has a longer lifetime and it is predominant for resonant interactions. Silica glass is a centrosymmetric material; therefore, second order nonlinear interactions are forbidden but third order parametric and non-parametric oscillations can be easily exploited in WGM microcavities. Previous works have been focused on toroidal WGMRs, where most of the excitable modes are constrained to be the equatorial ones [27], or on highly nonlinear materials [28,29]. We have explored efficient generation of visible light via third-harmonic generation (THG) and TSFG in silica microspherical WGMR.

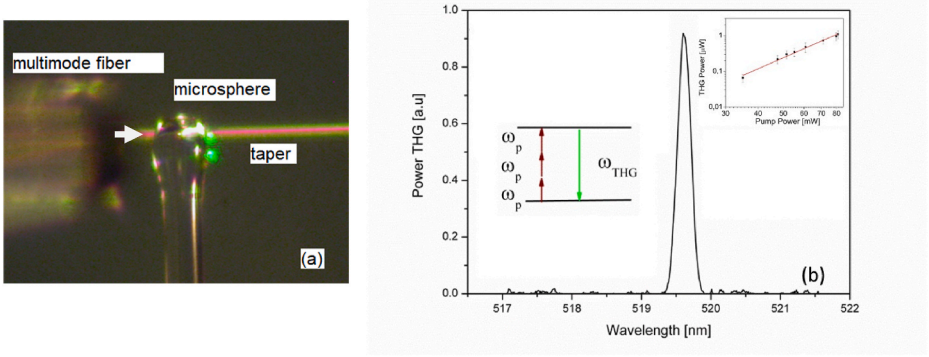

Fig. 3. a) Picture of a 57 μm in diameter microphere emitting two lobes in the green (TH) corresponding to a higher order polar WGM codirectional with the pump (white arrow). On the left side the MMF can be seen out of focus. b) Emission spectrum of TH at 519.6 nm when pumping at 1557 nm. The inset plots the TH power vs the launched pump power, with a linear fit having slope equal to 3.1 ± 0.1 (red line). (For interpretation of the references to color in this figure legend, the reader is referred to the Web version of this article.)

3.1. Third harmonic and sum frequency generation in silica microspheres

Phase and mode matching, energy conservation and high circulating intensities inside the resonator are the main ingredients for an efficient generation of visible light via third harmonic generation (THG) [30]. The frequency of the TH and of the pump are related by the energy conservation rule, i.e. $\omega_{THG} = 3\omega_P$, and can be fulfilled only if both ones fall within the WGM position with a tolerance of the order of the resonance linewidth. We demonstrated that the proper sphere diameter allows to satisfy this requirement [31]. Instead, phase matching condition, i.e. $n(\omega_{THG})=n(3\omega_P)$, can be fulfilled thanks to the compensation of linear and non-linear dispersion by degenerate WGMs dense distribution with different polar number m and decreasing effective index, inversely proportional to sphere radius R, $n_{eff}=m/kR$ [13]. Microspheres in the 25 ÷ 40 μm diameter range, with controlled size down to about 1%, and typical Q factors of the order of 10^7 were fabricated starting by a half-tapered fiber. This latter is obtained by heating and stretching an optical fiber and then, once it breaks, the tip is melted using the arc discharge of a commercial fusion splicer [17].

The experimental setup is based on a TDL (Photonetics Tunics, centered at 1570 nm) amplified by an EDFA (erbium-doped fiber amplifier, IPG Photonics EAD-2K–C), which passes through a polarization controller before it is coupled to the WGMR via a tapered fiber. The thermal self-locking of the WGM to the pump laser is obtained by tuning the laser into a resonance from high to low frequencies [32]. The light scattered from the microsphere surface is collected with a multimode fiber (MMF, 50 μm core, 0.2 NA) and the THG signals were detected on the OSA, as shown in Fig. 3a. A small portion of the TH signal was also coupled to the taper output even though the taper is not mode matched in the visible [33]. In Fig. 3b, a typical TH signal emission at 519.6 nm in a microsphere of 57 μm in diameter, pumped at the resonant wavelength of 1557 nm is shown. The expected cubic dependence of scattered visible light on the lunched pump power is plotted in the inset of Fig. 3b. A maximum THG signal (P_{TH}) of about 1 μW for scattered light and about 0.1 μW for fiber guided was obtained with a maximum launched pump power (P_p) of about 80 mW. Thus, a record maximum conversion efficiency η (P_{TH}/P_p) was in excess of 10^{-5} (10^{-6} in fiber signal).

In the most general case of TSFG, where input frequencies are not degenerate, three different waves interact with a nonlinear medium to generate a fourth wave of different frequency ($\omega_{TSFG} = \omega_1 + \omega_2 + \omega_3$). On the other hand, contrary to parametric effects, Raman scattering is a pure gain process and intrinsically phase-matched over the energy levels of the molecule. The Raman emission can be seen as a down-conversion of a pump photon and phonon associated with the vibrational mode of the molecule. In WGM silica microspheres, also cascaded Raman laser have been demonstrated [34]. In these oscillations, the Raman signals serve to secondary pump field and generate higher-order Raman waves. Increasing the pump power, the first Stokes line extracts power from the pump until it becomes strong enough to seed the next Stokes line generation. In the infrared region the cascaded SRS, as SRS, occurs as standing wave because the Raman gain is the same either for the forward or the backward traveling waves. In the presence of these phenomena, TSFG allows multicolor visible emissions (red, orange, yellow, and green) by tuning the pump wavelength. The spectra measured for each different color and the corresponding microsphere pictures are shown in Fig. 4.

3.2. Stimulated Brillouin scattering in silica microbubbles

Stimulated Brillouin Scattering (SBS) is a pure gain inelastic scattering process automatically phase-matched, resulting from the coherent interaction of acoustic phonons and light photons, which can be strongly enhanced by the WGMs. The WGM resonator acts as a dual photonic-phononic cavity due to the overlap of both waves inside it. The

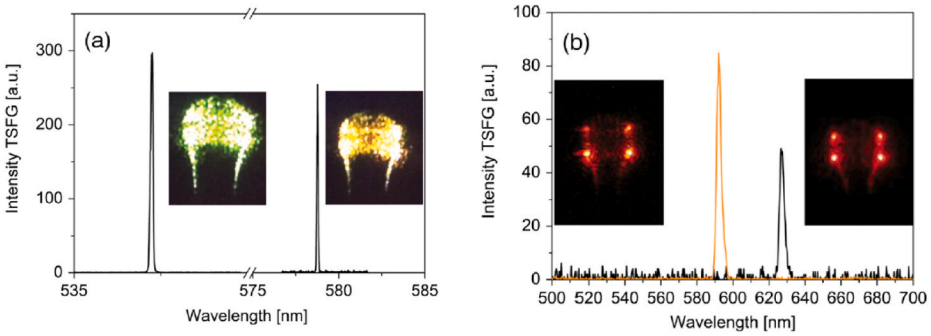

Fig. 4. Emission spectra indicating standing waves by the third order sum frequency generation among the pump wavelength and the cascaded Raman lines. (a) Left: at 1568.4 nm pump wavelength, emission at 537.24 nm; right: at 1567 nm pump wavelength, with emission at 578.76 nm; (b) Left: at 1553 nm pump wavelength, emitting at 592 nm; right: at 1568.4 nm pump wavelength, with emission at 625 nm [31].

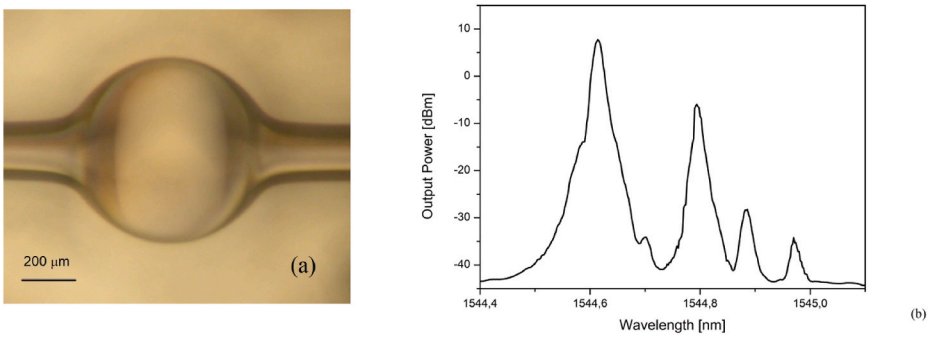

Fig. 5. a) Optical microscope image of a silica microbubble resonators obtained from commercial Postnova Z-FSS-200280 capillary. b) Fourth order cascaded SBS in forward direction for a MBR of diameter about 675 μm and wall thickness of about 2 μm, with $\lambda_p = 1544{,}614$.

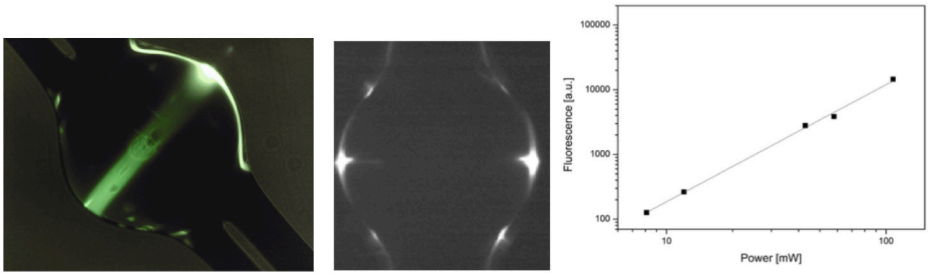

Fig. 6. a) Fluorescence image of the MBR filled with 10^{-3} fluorescein solution. b) Fluorescence image of the MBR filled with 10^{-6} solution of Rhodamine 6G. c) TPF signal versus the pump laser power in log-log scale with linear fit (slope close to 2) [50].

SBS has a large gain coefficients and very narrow gain bandwidth [30]. In silica, this bandwidth is of the order of a few tens of MHz at 10 GHz from the pump. Optimal criteria for SBS include that the free spectral range (FSR) of the resonator should exactly match the Brillouin frequency shift. This severe constraint on the cavity size [35–38], and consequently on the fabrication procedure, can be bypassed thanks to the strong eccentricity of microbubble resonator (MBR), which presents dense spectra of high order polar modes with a FSR smaller than that of the fundamental one [39]. MBRs with highly controllable sizes, like the one shown in Fig. 5a, were fabricated from pressurized silica capillaries (Postnova Z-FSS-200280) using two parallel arc discharges generated by a homemade four electrodes control system, which allows to uniformly melt their wall so that inner pressure can inflate the microbubble. The diameters range from a minimum of about 470 μm up to a maximum of about 700 μm, with 2 ÷ 3 μm wall thickness range and corresponding quality factors Q of about 3.5 x 10^7. Fig. 5b shows the results achieved using an experimental setup similar to that presented in the previous section, and launching a pump power up to 200 mW in a MBR of about 675 μm diameter and 2 μm wall thickness. We have experimentally shown that MBRs of large diameters and thin walls can enhance the Brillouin lasing efficiency, both in forward and backward directions, with a cascade up to the 4th order.

Even and odd orders are observed in both directions, showing even (odd) orders more lasing efficient in forward (backward) direction [23,40]. The related Stokes lines are shifted by 90, 180, 260 and 350 p.m. for a 1544,614 nm pump wavelength. Similarly to microbubbles resonators [41,42], SBS has been also demonstrated in silica microbottles [35] and in silica [43,44] and tellurite [45] microspheres.

4. Two-photon fluorescence in microbubble resonators

Two-Photon Fluorescence (TPF) is a validated technique for imaging and detection of labeled biological material [46–48], which has numerous advantages over conventional one photon fluorescence (OPF), but requires high photon density flux, reached by tightly focusing the laser light. In many cases, resonators are used to avoid tight focusing and achieve the needed intensities [49]. MBR filled with appropriate liquids are the most suitable WGMR for TPF. In Ref. [50], we demonstrated TPF filling MBR with a 10^{-3} and 10^{-4} fluorescein and 10^{-6} Rhodamine 6G solutions. We used a modified confocal microscope – pumped by a Coherent Mira 900- Ti:Sapphire (with a repetition rate 76 MHz and 150 fs pulse duration) – for coupling the light into the microbubble resonator [51]. The laser has an average power of 1.2 W and the wavelength was set to 800 nm. The two-photon absorption spectra of many fluorophores [52] falls within the tunable range of Ti:Sapphire laser (690–950 nm). The laser beam was coupled into the MBR by focusing it tangential to the resonator wall through two different dry objectives, namely 4X and 10X and 0.5 NA. The excitation light was filtered by a dichroic mirror Semrock FF720-SDi01 and a filter Schott BG39. Fig. 6a shows the TPF emission of the MBR filled with 10^{-3} solution of fluorescein, on a band around the equatorial plane, partially coupled back to the bubble walls. TPF signal from a Rhodamine 6G filled microbubble, for an incident power of about 190 mW at 800 nm, and its logarithmic representation versus incident laser power, are shown in Fig. 6b and c, respectively. The two-photon signal was validated by checking its quadratic dependence on the excitation laser power.

5. Non-linear Kerr switching microdevices

All-optical switching at low powers in high Q-factor silica microspheres coated by a Kerr material was theoretically proposed in Ref. [53], while switching with conjugated polymer was provided in Ref. [54], but by means of thermo-optic effect. Large refractive index changes can be easily obtained on picosecond time scales, thanks to the electronic Kerr effect in WGMRs, using intensities well below the damage thresholds of the polymers [55,56]. A strong third order optical nonlinearity is required for optically induced refractive index (RI) changes. The material refractive index n and the absorption coefficient α, depend on the light intensity I as $n = n_0 + n_2 I + n_4 I^2 + \ldots$, where n_2 and n_4 are the nonlinear RIs (related respectively to $\chi^{(3)}$ and $\chi^{(5)}$, the third

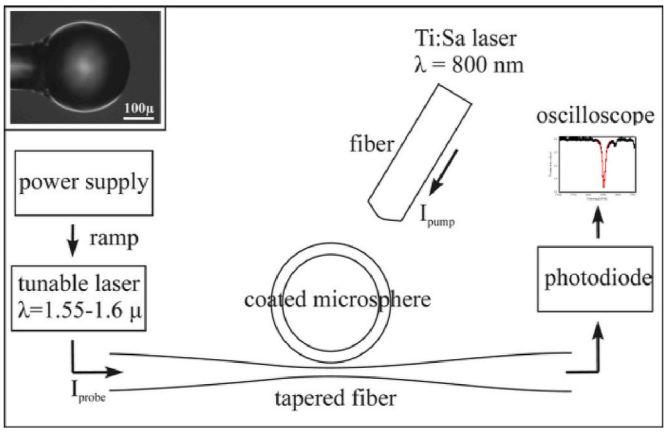

Fig. 7. Experimental pump-and-probe set-up. Left hand side inset: optical image of the WGM microsphere resonator. Right hand side inset: typical resonance [60].

and fifth order nonlinear optical susceptibility) and $\alpha = \alpha_0 + \beta I$, where β is the nonlinear absorption coefficient. If the $\chi^{(3)}$ and $\chi^{(5)}$ are due to the fast electronic Kerr nonlinearity, then the switching has a picosecond time scale, which represents the most desirable working condition. Two different types of switching for the observed signal can be achieved: only one light beam, which undergoes self-switching between high and low intensity levels [57,58] or two light beams of different wavelengths with intensities I_{probe} and I_{pump}. In this last case, the resonant conditions for the *probe* beam depends on the *pump* beam [54].

We demonstrated, in silica microspheres, the first evidence for all optical switching of WGMs based on third order Kerr non-linearity in a thin polymer layer [59,60]. We have chosen as material a polyfluorene derivative, PF(o)n, functionalised at the C9 position of the fluorine ring with two pendant octyl chains [59]. The linear absorption has a peak around 379 nm [59]. PF(o) layer of about 100 nm thickness were obtained by means of the dip coating technique. In the experimental setup, shown in Fig. 7, the light I_{probe} is coupled to the Kerr-polymer coated WGMR by a tapered fibre and, at the same time, the WGMR is illuminated by a pump light I_{pump}. Both light beams, I_{probe} and I_{pump}, interact with the resonator and the WGM, excited by the probe beam, is detuned by the pump beam. The transmission spectrum of the WGMR microresonator was observed using, as a probe, a tunable external-cavity laser (Tunics Plus) at 1500–1670 nm wavelength range, with 300 kHz linewidth. The PF(o)n-coated spheres were then illuminated by I_{pump}, from an ultrafast Ti:Sapphire laser (Mira 900F, Coherent). The ultrafast radiation was coupled to a single mode fiber (SM800, Fibercore) with a lensed distal end, which was placed at about 1 mm from the microresonator surface.

A quadratic dependency (due to two-photon absorption, TPA) of the frequency shift versus pump power was observed for $l_{probe} = 1558$ nm and $l_{pump} = 775$ nm, as shown in Fig. 8a. A maximum detuning of 3 GHz was obtained with an average pump power of 25 mW. In order to better discriminate the role of the thermal shift from the Kerr shift, we performed pump and probe measurements both in the CW and pulsed regimes for the same range of the average pump power. We obtained a much lower spectral shift in the CW regime as compared to the pulsed one. Fig. 8a also shows a frequency shift of up to 0.5 GHz obtained in the mode-locked regime at 825 nm, which is far from the second harmonic of the probe beam and allows avoiding TPA [59]. At $l_{pump} = 825$ nm the dependency is linear and the detuning is the same of the CW regime, indicating that in the absence of TPA, the pump acts as a thermal source. We also tested microspheres coated with a layer of inert polymer, i.e. Eudragit ®L100 [61]. The WGM detuning as a function of the pump power was nearly the same for mode-locked pump laser regime and for CW one, with an almost null red-shift up to 20 mW of pump power.

6. Conclusions

We reviewed several significant results we obtained on lasing and non-linear effects in WGM glass microresonators. We have exploited Er^{3+}-doped silica and phosphate glass microspheres as micro-laser sources with a tunability in excess of 30 nm around 1550 nm. Efficient THG in silica microspheres was demonstrated by properly choosing the resonator size and the excited WGMs for fulfilling energy conservation and phase matching conditions. Fourth order cascaded SBS was observed in silica microbubbles exploiting their dense resonance spectra, which allow to efficiently match the narrow Brillouin bandwidth. Two-photon fluorescence in hollow WGMR filled with fluorescein or Rhodamine was demonstrated, showing quadratic dependence on the excitation laser power. Finally, we demonstrated all-optical switching on a WGMR coated by a polyfluorene thin layer. Resonant frequency shifts of 3 GHz were observed under pulsed optical pumping showing great potential of conjugated polymers for realizing nonlinear switching.

CRediT authorship contribution statement

D. Farnesi: Writing – original draft, Investigation. **S. Berneschi:** Investigation. **G. Frigenti:** Investigation. **G. Nunzi Conti:** Writing – original draft, Methodology, Supervision. **S. Pelli:** Methodology, Investigation. **P. Feron:** Conceptualization, Formal analysis. **T. Murzina:** Methodology, Supervision. **M. Ferrari:** Methodology, Supervision. **S. Soria:** Methodology, Investigation, Supervision.

Declaration of competing interest

The authors declare that they have no known competing financial

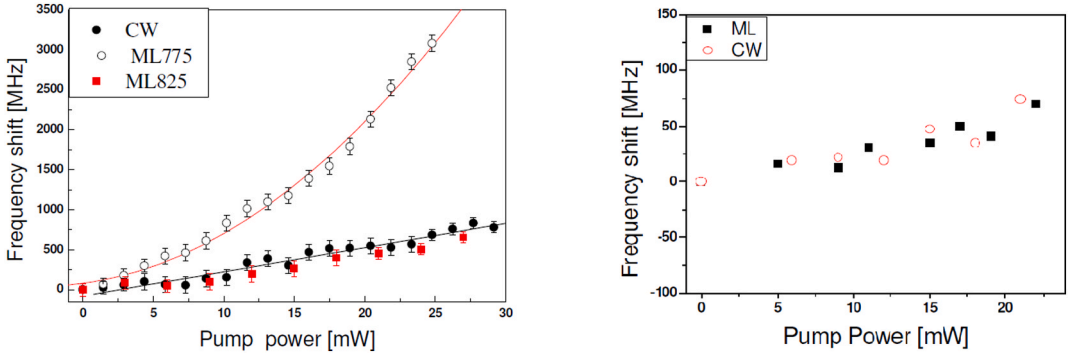

Fig. 8. a). Pump power dependence of the detuning of WGM in PF(o)n coated microspheres for mode-locked Ti-sapphire pump laser for two different regimes: CW (filled circles), mode locked at 775 nm (empty circles) and at 825 nm. b) Eudragit coated microspheres for CW (empty circles) and pulsed (filled squares) pump laser. The probe wavelength is set at 1558 nm [60].

interests or personal relationships that could have appeared to influence the work reported in this paper.

Acknowledgments

We thank Mr. Franco Cosi from CNR-IFAC for taper fabrication. This research study was partially supported by the CNR-RFBR bilateral project “Active Resonant Tunable Dielectric Microstructures for Ultra-fast Photonics” (RFBR grant No 20-52-7818).

References

[1] V.B. Braginsky, M.L.G. Gorodetsky, V.S. Ilchenko, Quality-factor and nonlinear properties of optical whispering-gallery modes, Phys. Lett. 137 (1989) 393–397, https://doi.org/10.1016/0375-9601(89)90912-2.
[2] L. He, Ş.K. Özdemir, L. Yang, Whispering gallery microcavity lasers: WGM microlasers, Laser Photon. Rev. 7 (2013) 60–82, https://doi.org/10.1002/lpor.201100032.
[3] A. Fernandez-Bravo, K. Yao, E.S. Barnard, N.J. Borys, E.S. Levy, B. Tian, C.A. Tajon, L. Moretti, M.V. Altoe, S. Aloni, K. Beketayev, F. Scotognella, B.E. Cohen, E. M. Chan, P.J. Schuck, Continuous-wave upconverting nanoparticle microlasers, Nat. Nanotechnol. 13 (2018) 572–577, https://doi.org/10.1038/s41565-018-0161-8.
[4] G. Lin, A. Coillet, Y.K. Chembo, Nonlinear photonics with high-Q whispering-gallery-mode resonators, Adv. Opt Photon 9 (2017) 828–890, https://doi.org/10.1364/AOP.9.000828.
[5] M. Aspelmeyer, T.J. Kippenberg, F. Marquardt (Eds.), Cavity Optomechanics: Nano- and Micromechanical Resonators Interacting with Light, Springer-Verlag, Berlin Heidelberg, 2014, https://doi.org/10.1007/978-3-642-55312-7.
[6] M.R. Foreman, J.D. Swaim, F. Vollmer, Whispering gallery mode sensors, Adv. Opt. Photon., AOP 7 (2015) 168–240, https://doi.org/10.1364/AOP.7.000168.
[7] K.D. Heylman, K.A. Knapper, E.H. Horak, M.T. Rea, S.K. Vanga, R.H. Goldsmith, Optical microresonators for sensing and transduction: a materials perspective, Adv. Mater. 29 (2017), https://doi.org/10.1002/adma.201700037.
[8] G. Palma, M.C. Falconi, F. Starecki, V. Nazabal, T. Yano, T. Kishi, T. Kumagai, F. Prudenzano, Novel double step approach for optical sensing via microsphere WGM resonance, Opt. Express, OE 24 (2016) 26956–26971, https://doi.org/10.1364/OE.24.026956.
[9] A. Pasquazi, M. Peccianti, L. Razzari, D.J. Moss, S. Coen, M. Erkintalo, Y. K. Chembo, T. Hansson, S. Wabnitz, P. Del’Haye, X. Xue, A.M. Weiner, R. Morandotti, Micro-combs: a novel generation of optical sources, Phys. Rep. 729 (2018) 1–81, https://doi.org/10.1016/j.physrep.2017.08.004.
[10] G. Frigenti, M. Arjmand, A. Barucci, F. Baldini, S. Berneschi, D. Farnesi, M. Gianfreda, S. Pelli, S. Soria, A. Aray, others, Coupling analysis of high Q resonators in add-drop configuration through cavity ringdown spectroscopy, J. Opt. 20 (2018), 065706.
[11] R.E. Benner, P.W. Barber, J.F. Owen, R.K. Chang, Observation of structure resonances in the fluorescence spectra from microspheres, Phys. Rev. Lett. 44 (1980) 4.
[12] C.G.B. Garrett, W. Kaiser, W.L. Bond, Stimulated emission into optical whispering modes of spheres, Phys. Rev. 124 (1961) 1807–1809, https://doi.org/10.1103/PhysRev.124.1807.
[13] A. Chiasera, Y. Dumeige, P. Féron, M. Ferrari, Y. Jestin, G. Nunzi Conti, S. Pelli, S. Soria, G.c. Righini, Spherical whispering-gallery-mode microresonators, Laser Photon. Rev. 4 (2010) 457–482, https://doi.org/10.1002/lpor.200910016.
[14] M. Sumetsky, Y. Dulashko, R.S. Windeler, Optical microbubble resonator, Opt. Lett., OL 35 (2010) 898–900, https://doi.org/10.1364/OL.35.000898.
[15] P. Bianucci, Optical microbottle resonators for sensing, Sensors 16 (2016) 1841, https://doi.org/10.3390/s16111841.
[16] S.V. Suchkov, M. Sumetsky, A.A. Sukhorukov, Frequency comb generation in SNAP bottle resonators, Opt. Lett. 42 (2017) 2149, https://doi.org/10.1364/OL.42.002149.
[17] M. Brenci, R. Calzolai, F. Cosi, G.N. Conti, S. Pelli, G.C. Righini, Microspherical resonators for biophotonic sensors, in: Lightmetry and Light and Optics in Biomedicine 2004, SPIE, 2006, pp. 225–233, https://doi.org/10.1117/12.675800.
[18] S. Berneschi, D. Farnesi, F. Cosi, G.N. Conti, S. Pelli, G. Righini, S. Soria, High Q silica microbubble resonators fabricated by arc discharge, Opt Lett. 36 (2011) 3521–3523.
[19] G. Palma, M.C. Falconi, F. Starecki, V. Nazabal, J. Ari, L. Bodiou, J. Charrier, Y. Dumeige, E. Baudet, F. Prudenzano, Design of praseodymium-doped chalcogenide micro-disk emitting at 4.7um, Opt. Express, OE 25 (2017) 7014–7030, https://doi.org/10.1364/OE.25.007014.
[20] B. Way, R.K. Jain, M. Hossein-Zadeh, High-Q microresonators for mid-IR light sources and molecular sensors, Opt. Lett., OL 37 (2012) 4389–4391, https://doi.org/10.1364/OL.37.004389.
[21] C. Grillet, S.N. Bian, E.C. Magi, B.J. Eggleton, Fiber taper coupling to chalcogenide microsphere modes, Appl. Phys. Lett. 92 (2008) 171109, https://doi.org/10.1063/1.2918128.
[22] F. Lissillour, D. Messager, G. Stéphan, P. Féron, Whispering-gallery-mode laser at 1.56 μm excited by a fiber taper, Opt. Lett., OL 26 (2001) 1051–1053, https://doi.org/10.1364/OL.26.001051.
[23] X. Roselló-Mechó, D. Farnesi, G. Frigenti, A. Barucci, A. Fernández-Bienes, T. García-Fernández, F. Ratto, M. Delgado-Pinar, M.V. Andrés, G.N. Conti, others, Parametrical optomechanical oscillations in PhoXonic whispering gallery mode resonators, Sci. Rep. 9 (2019) 1–7.
[24] G. Nunzi Conti, A. Chiasera, L. Ghisa, S. Berneschi, M. Brenci, Y. Dumeige, S. Pelli, S. Sebastiani, P. Feron, M. Ferrari, G.C. Righini, Spectroscopic and lasing properties of Er3+-doped glass microspheres, J. Non-Cryst. Solids 352 (2006) 2360–2363, https://doi.org/10.1016/j.jnoncrysol.2006.01.089.
[25] D. Ristić, S. Berneschi, M. Camerini, D. Farnesi, S. Pelli, C. Trono, A. Chiappini, A. Chiasera, M. Ferrari, A. Lukowiak, Y. Dumeige, P. Féron, G.C. Righini, S. Soria, G.N. Conti, Photoluminescence and lasing in whispering gallery mode glass microspherical resonators, J. Lumin. 170 (2016) 755–760, https://doi.org/10.1016/j.jlumin.2015.10.050.
[26] F. Lissillour, P. Féron, N. Dubreuil, P. Dupriez, M. Poulain, G.M. Stéphan, Erbium-doped microspherical lasers at 1.56 μm, Electron. Lett. 36 (2000) 1382–1384, https://doi.org/10.1049/el:20001012.
[27] T. Carmon, K.J. Vahala, Visible continuous emission from a silica microphotonic device by third-harmonic generation, Nat. Phys. 3 (2007) 430–435, https://doi.org/10.1038/nphys601.
[28] S.-X. Qian, R.K. Chang, Multiorder Stokes emission from micrometer-size droplets, Phys. Rev. Lett. 56 (1986) 926–929, https://doi.org/10.1103/PhysRevLett.56.926.
[29] H.-B. Lin, A.J. Campillo, Cw nonlinear optics in droplet microcavities displaying enhanced gain, Phys. Rev. Lett. 73 (1994) 2440–2443, https://doi.org/10.1103/PhysRevLett.73.2440.
[30] R.W. Boyd, Nonlinear Optics, third ed., Academic Press, Inc., USA, 2008.
[31] D. Farnesi, A. Barucci, G. Righini, S. Berneschi, S. Soria, G.N. Conti, Optical frequency conversion in silica-whispering-gallery-mode microspherical resonators, Phys. Rev. Lett. 112 (2014), 093901.
[32] T. Carmon, L. Yang, K.J. Vahala, Dynamical thermal behavior and thermal self-stability of microcavities, Opt. Express, OE 12 (2004) 4742–4750, https://doi.org/10.1364/OPEX.12.004742.
[33] D. Farnesi, A. Barucci, S. Berneschi, G.C. Righini, S. Soria, G.N. Conti, Multicolour emission in silica whispering gallery mode microspherical resonators, in: Laser Resonators, Microresonators, and Beam Control XVI, International Society for Optics and Photonics, 2014, p. 896008.
[34] B. Min, T.J. Kippenberg, K.J. Vahala, Compact, fiber-compatible, cascaded Raman laser, Opt. Lett., OL 28 (2003) 1507–1509, https://doi.org/10.1364/OL.28.001507.
[35] M. Asano, Y. Takeuchi, S.K. Ozdemir, R. Ikuta, L. Yang, N. Imoto, T. Yamamoto, Stimulated Brillouin scattering and Brillouin-coupled four-wave-mixing in a silica microbottle resonator, Opt. Express, OE 24 (2016) 12082–12092, https://doi.org/10.1364/OE.24.012082.
[36] M. Asano, S. Komori, R. Ikuta, N. Imoto, Ş.K. Özdemir, T. Yamamoto, Visible light emission from a silica microbottle resonator by second- and third-harmonic generation, Opt. Lett., OL 41 (2016) 5793–5796, https://doi.org/10.1364/OL.41.005793.
[37] I.S. Grudinin, A.B. Matsko, L. Maleki, Brillouin lasing with a CaF2 whispering gallery mode resonator, Phys. Rev. Lett. 102 (2009), 043902, https://doi.org/10.1103/PhysRevLett.102.043902.
[38] B.J. Eggleton, C.G. Poulton, R. Pant, Inducing and harnessing stimulated Brillouin scattering in photonic integrated circuits, Adv. Opt. Photon., AOP 5 (2013) 536–587, https://doi.org/10.1364/AOP.5.000536.
[39] D. Farnesi, A. Barucci, G.C. Righini, G.N. Conti, S. Soria, Generation of hyper-parametric oscillations in silica microbubbles, Opt Lett. 40 (2015) 4508–4511.
[40] D. Farnesi, G. Righini, G.N. Conti, S. Soria, Efficient frequency generation in phoxonic cavities based on hollow whispering gallery mode resonators, Sci. Rep. 7 (2017) 1–6.
[41] Q. Lu, S. Liu, X. Wu, L. Liu, L. Xu, Stimulated Brillouin laser and frequency comb generation in high-Q microbubble resonators, Opt. Lett., OL 41 (2016) 1736–1739, https://doi.org/10.1364/OL.41.001736.
[42] G. Bahl, K.H. Kim, W. Lee, J. Liu, X. Fan, T. Carmon, Brillouin cavity optomechanics with microfluidic devices, Nat. Commun. 4 (2013) 1994, https://doi.org/10.1038/ncomms2994.
[43] G. Bahl, J. Zehnpfennig, M. Tomes, T. Carmon, Stimulated optomechanical excitation of surface acoustic waves in a microdevice, Nat. Commun. 2 (2011) 403, https://doi.org/10.1038/ncomms1412.
[44] M. Tomes, T. Carmon, Photonic micro-electromechanical systems vibrating at $X $-band (11-GHz) rates, Phys. Rev. Lett. 102 (2009) 113601, https://doi.org/10.1103/PhysRevLett.102.113601.
[45] C. Guo, K. Che, P. Zhang, J. Wu, Y. Huang, H. Xu, Z. Cai, Low-threshold stimulated Brillouin scattering in high-Q whispering gallery mode tellurite microspheres, Opt. Express, OE 23 (2015) 32261–32266, https://doi.org/10.1364/OE.23.032261.
[46] A. Selle, C. Kappel, M.A. Bader, G. Marowsky, K. Winkler, U. Alexiev, Picosecond-pulse-induced two-photon fluorescence enhancement in biological material by application of grating waveguide structures, Opt. Lett., OL 30 (2005) 1683–1685, https://doi.org/10.1364/OL.30.001683.
[47] A.T.K. N, A. Muriano, J.-P. Salvador, R. Galve, M.P. Marco, D. Zalvidea, P. Loza-Alvarez, T. Katchalski, E. Grinvald, A.A. Friesem, S. Soria, Nonlinear immunofluorescent assay for androgenic hormones based on resonant structures, Opt. Express, OE 16 (2008) 13315–13322, https://doi.org/10.1364/OE.16.013315.
[48] A. Muriano, K.N.A. Thayil, J.-P. Salvador, P. Loza-Alvarez, S. Soria, R. Galve, M.-P. Marco, Two-photon fluorescent immunosensor for androgenic hormones using resonant grating waveguide structures, Sensor. Actuator. B Chem. 174 (2012) 394–401, https://doi.org/10.1016/j.snb.2012.08.006.

[49] G.A. Cohoon, K. Kieu, R.A. Norwood, Observation of two-photon fluorescence for Rhodamine 6G in microbubble resonators, Opt. Lett., OL 39 (2014) 3098–3101, https://doi.org/10.1364/OL.39.003098.
[50] C. Pastells, M.-P. Marco, D. Merino, P. Loza-Alvarez, L. Pasquardini, L. Lunelli, C. Pederzolli, N. Daldosso, D. Farnesi, S. Berneschi, others, Two photon versus one photon fluorescence excitation in whispering gallery mode microresonators, J. Lumin. 170 (2016) 860–865.
[51] L.L. Martín, P. Haro-González, I.R. Martín, D. Navarro-Urrios, D. Alonso, C. Pérez-Rodríguez, D. Jaque, N.E. Capuj, Whispering-gallery modes in glass microspheres: optimization of pumping in a modified confocal microscope, Opt. Lett., OL 36 (2011) 615–617, https://doi.org/10.1364/OL.36.000615.
[52] F. Bestvater, E. Spiess, G. Stobrawa, M. Hacker, T. Feurer, T. Porwol, U. Berchner-Pfannschmidt, C. Wotzlaw, H. Acker, Two-photon fluorescence absorption and emission spectra of dyes relevant for cell imaging, J. Microsc. 208 (2002) 108–115, https://doi.org/10.1046/j.1365-2818.2002.01074.x.
[53] M. Haraguchi, M. Fukui, Y. Tamaki, T. Okamoto, Optical switching due to whispering gallery modes in dielectric microspheres coated by a Kerr material, J. Microsc. 210 (2003) 229–233, https://doi.org/10.1046/j.1365-2818.2003.01150.x.
[54] H.C. Tapalian, J.-P. Laine, P.A. Lane, Thermooptical switches using coated microsphere resonators, IEEE Photon. Technol. Lett. 14 (2002) 1118–1120, https://doi.org/10.1109/LPT.2002.1021988.
[55] M.A. Bader, G. Marowsky, A. Bahtiar, K. Koynov, C. Bubeck, H. Tillmann, H.-H. Hörhold, S. Pereira, Poly(p-phenylenevinylene) derivatives: new promising materials for nonlinear all-optical waveguide switching, J. Opt. Soc. Am. B, JOSAB 19 (2002) 2250–2262, https://doi.org/10.1364/JOSAB.19.002250.
[56] D.J.W. Paras N. Prasad, Introduction to Nonlinear Optical Effects in Molecules and Polymers, John Wiley & Sons, New York, 1991, https://doi.org/10.1002/pi.4990250317. Polymer International. 25 (1991) 199–199.
[57] F. Treussart, V.S. Ilchenko, J.-F. Roch, J. Hare, V. Lefèvre-Seguin, J.-M. Raimond, S. Haroche, Evidence for intrinsic Kerr bistability of high-Q microsphere resonators in superfluid helium, Eur. Phys. J. D. 1 (1998) 235–238, https://doi.org/10.1007/PL00021556.
[58] M. Pöllinger, A. Rauschenbeutel, All-optical signal processing at ultra-low powers in bottle microresonators using the Kerr effect, Opt. Express, OE 18 (2010) 17764–17775, https://doi.org/10.1364/OE.18.017764.
[59] L.S. Chinelatto, J. del Barrio, M. Piñol, L. Oriol, M.A. Matranga, M.P. De Santo, R. Barberi, Oligofluorene blue emitters for cholesteric liquid crystal lasers, J. Photochem. Photobiol. Chem. 210 (2010) 130–139, https://doi.org/10.1016/j.jphotochem.2010.01.006.
[60] I. Razdolskiy, S. Berneschi, G.N. Conti, S. Pelli, T.V. Murzina, G.C. Righini, S. Soria, Hybrid microspheres for nonlinear Kerr switching devices, Opt. Express, OE 19 (2011) 9523–9528, https://doi.org/10.1364/OE.19.009523.
[61] T.V. Murzina, G.N. Conti, A. Barucci, S. Berneschi, I. Razdolskiy, S. Soria, Kerr versus thermal non-linear effects studied by hybrid whispering gallery mode resonators [Invited], Opt. Mater. Express, OME 2 (2012) 1088–1094, https://doi.org/10.1364/OME.2.001088.